



1 **Parametrization consequences of constraining soil organic**  
2 **matter models by total carbon and radiocarbon using long-**  
3 **term field data**

4

5 **L. Menichetti<sup>1</sup>, T. Kätterer<sup>2</sup> and J. Leifeld<sup>1</sup>**

6 [1]{ Agroscope, Climate / Air Pollution Group, Reckenholzstrasse 191, CH 8046 Zürich,  
7 Switzerland }

8 [2]{Swedish University of Agricultural Sciences (SLU), Department of Ecology, Box 7044,  
9 75007 Uppsala, Sweden }

10 Correspondence to: L. Menichetti (Lorenzo.Menichetti@agroscope.admin.ch)

11

12 **Abstract**

13 Soil organic carbon (SOC) dynamics result from different interacting processes and controls  
14 on spatial scales from sub-aggregate to pedon to the whole ecosystem. These complex  
15 dynamics are translated into models as abundant degrees of freedom. This high number of not  
16 directly measurable variables and, on the other hand, very limited data at disposal result in  
17 equifinality and parameter uncertainty.

18 Carbon radioisotope measurements are a proxy for SOC age both at annual to decadal (bomb  
19 peak based) and centennial to millennial time scales (radio decay based), and thus can be used  
20 in addition to total organic C for constraining SOC models. By considering this additional  
21 information, uncertainties in model structure and parameters may be reduced.

22 To test this hypothesis we studied SOC dynamics and their defining kinetic parameters in the  
23 ZOFÉ experiment, a >60-years old controlled cropland experiment in Switzerland, by  
24 utilising SOC and SO<sup>14</sup>C time-series. To represent different processes we applied five model  
25 structures, all stemming from a simple mother model (ICBM): I) two decomposing pools, II)  
26 an inert pool added, III) three decomposing pools, IV) two decomposing pools with a  
27 substrate control feedback on decomposition, V) as IV but with also an inert pool. These  
28 structures were extended to explicitly represent total SOC and <sup>14</sup>C pools.



1 The use of different model structures allowed us to explore model structural uncertainty and  
2 the impact of  $^{14}\text{C}$  on kinetic parameters. We considered parameter uncertainty by calibrating  
3 in a formal Bayesian framework.

4 By varying the relative importance of total SOC and  $\text{SO}^{14}\text{C}$  data in the calibration, we could  
5 quantify the effect of the information from these two data streams on estimated model  
6 parameters. The weighing of the two data streams was crucial for determining model  
7 outcomes, and we suggest including it in future modelling efforts whenever  $\text{SO}^{14}\text{C}$  data are  
8 available.

9 The measurements and all model structures indicated a dramatic decline in SOC in the ZOFÉ  
10 experiment after an initial land use change in 1949 from grass- to cropland, followed by a  
11 constant but smaller decline. According to all structures, the three treatments (control, mineral  
12 fertilizer, farmyard manure) we considered were still far from equilibrium. The estimates of  
13 mean residence time (MRT) of the C pools defined by our models were sensitive to the  
14 consideration of the  $\text{SO}^{14}\text{C}$  data stream. Model structure had a smaller effect on estimated  
15 MRT, which ranged between 5.91 and 4.22 years and 78.93 and 98.85 years for young and  
16 old pool, respectively, for structures without substrate interactions.

17 The simplest model structure performed the best according to information criteria, validating  
18 the idea that we still lack data for mechanistic SOC models. Although we could not exclude  
19 any of the considered processes possibly involved in SOC decomposition, it was not possible  
20 to discriminate their relative importance.

21

## 22 **1 Introduction**

23 The dynamics of soil organic carbon (SOC) are directly linked to major soil ecosystem  
24 services such as soil fertility, resistance to erosion, C sequestration and soil  $\text{CO}_2$  emissions  
25 (Lal, 2004). Understanding such dynamics is therefore of paramount importance for the  
26 challenges of the present century (IPCC, 2014). In particular, the precise quantification of  
27 SOC cycles would allow for a monetization of the respective ecosystem services, and is a  
28 crucial step to overcome the failure of this market (Alexander *et al.*, 2015).

29 However, the time scale of SOC decomposition, from years to millennia, makes it difficult to  
30 design experiments and requires gathering indirect answers through analysis of monitoring  
31 programs, long-term experiments and SOC turnover models. Most of these models, for



1 example among the most well-known RothC (Coleman *et al.*, 1997), Century (Parton *et al.*,  
2 1993) and Yasso (Liski *et al.*, 2005), are built around multiple conceptual pools decomposing  
3 with first-order kinetics. This basic structure works well to simulate decadal to centennial  
4 time scales, but shows problems with longer (when considering more protected organic  
5 matter, e.g. Trumbore and Czimczik, 2008) or shorter (when considering microbial dynamics,  
6 e.g. Schimel and Weintraub, 2003) time scales.

7 Formally, these models could be extended in complexity to represent more accurately all the  
8 processes involved in SOC decomposition that we are aware of. However, a purely  
9 mechanistic modelling approach often fails because the lack of data in respect to the  
10 complexity of the system limits the number of latent variables (all the variables that cannot be  
11 directly measured) that we can infer. A high system complexity, as characterised by multiple  
12 interactions between parameters, causes equifinality problems (Beven, 2006). Representing  
13 such interactions in a way that is both accurate and abstract enough to realistically consider  
14 the availability of data is termed the bias/variance dilemma (Briscoe and Feldman, 2011).  
15 This dilemma represents the most critical point in producing reliable estimates in SOC  
16 modelling.

17 The struggle of contemporary SOC models becomes more evident when including  $\text{SO}^{14}\text{C}$   
18 data. When time series for both total SOC and  $\text{SO}^{14}\text{C}$  are available, they may suggest  
19 contradictory dynamics (Shirato *et al.*, 2013). This confirms the high uncertainty in defining  
20 contemporary SOC model structures and at the same time raises the question of how to use  
21 these two sources of information.

22 Methods for the inclusion of radiocarbon measurements in SOC models are currently actively  
23 developed. While most SOC models consider  $^{14}\text{C}$  implicitly through the use of mass balance  
24 equations, some attempts have been made to consider  $^{14}\text{C}$  explicitly (Ahrens *et al.*, 2014) as a  
25 separate set of C molecules. A similar approach has been proposed also for  $^{13}\text{C}$  by Ågren *et al.*  
26 (1996). The explicit approach offers more flexibility in the representation of processes that  
27 might influence  $\text{SO}^{14}\text{C}$  at the price of a minimal increase in model complexity. Nevertheless,  
28 even with explicit consideration of  $^{14}\text{C}$ , modelling results are still not well determined  
29 (Ahrens *et al.*, 2014).

30 Yet a few studies have considered  $\text{SO}^{14}\text{C}$  data within an uncertainty analysis framework.  
31 Braakhekke *et al.* (2014) and Ahrens *et al.* (2014) both considered model uncertainty, but  
32 focused on a single model structure. However, both parameter uncertainty and structural



1 uncertainty are significant problems endemic to environmental models (Beven, 2002).  
2 Moreover, in both these studies the model sensitivity to radiocarbon was limited to two cases,  
3 either including or excluding  $\text{SO}^{14}\text{C}$  data. The inclusion of  $\text{SO}^{14}\text{C}$  data can modify the model  
4 space substantially (Ahrens *et al.*, 2014) and in a non-linear way. The weight assigned to  
5  $\text{SO}^{14}\text{C}$  and SOC is a crucial parameter influencing strongly the modelling results, and the  
6 effect of this parameter should, therefore, be studied more in detail.

7 In order to consider the effect of  $^{14}\text{C}$  data with respect to structural uncertainty, we calibrated  
8 a set of SOC models over total SOC time series from the ZOFÉ long-term field experiment  
9 (Oberholzer *et al.*, 2014). In addition, we made use of  $\text{SO}^{14}\text{C}$  measurements in key positions  
10 of the time series. Model structures were built around ICBM, a basic two-pool SOC  
11 decomposition model (Andrén and Kätterer, 1997), and calibrated within a Markov chain  
12 Monte Carlo framework to take care of equifinality and parameter uncertainty. We considered  
13 the possibility of substrate interactions by introducing a control term on decomposition  
14 influenced by the amount of fresh substrate available. To consider the effect of total SOC and  
15  $\text{SO}^{14}\text{C}$  on the calibration, we assigned a relative weight to the two data streams and calibrated  
16 model structures across a gradient of such weights.

17 The three research questions driving this work are:

- 18 • How will the inclusion of  $^{14}\text{C}$  data influence the SOC parameters estimated from a multi-  
19 pool model?
- 20 • What are the reasons for the observed discrepancy between modelled total SOC and  
21  $\text{SO}^{14}\text{C}$  dynamics, and which are the most important ones?
- 22 • Can we model SOC and  $\text{SO}^{14}\text{C}$  jointly in a way that is minimalistic and flexible and yet  
23 effective?

24 These research questions generated the following, partially concurrent, hypotheses:

- 25 1. An underestimation of the age of slow C due to the presence of recalcitrant C (e.g.  
26 black C, Leifeld, 2008) or C protected through some other mechanisms is one possible reason  
27 for the observed discrepancy between SOC and  $\text{SO}^{14}\text{C}$  modelled kinetics. Thus, representing  
28 such slow C in the model as inert or particularly slow pool will improve model performances.
- 29 2. An interaction between substrate pools is a process often neglected in C models but  
30 which can contribute the observed discrepancy. Representing this process in the model can  
31 improve model performances.



1 3. Is it possible to discriminate between the above mentioned processes?

2 To answer our questions we compared the results from different model structures, each  
3 focusing on slightly different processes. By comparing different model structures we also  
4 aimed at understanding more realistically SOC kinetics in the ZOFÉ experiments by  
5 acknowledging some model structural uncertainty.

6

## 7 **2 Material and methods**

### 8 **2.1 Experimental site**

9 The data utilized in this study have been collected in the Zürich Organic Fertilization  
10 Experiment (ZOFÉ, Oberholzer et al. 2014), located in Switzerland at the Agroscope  
11 premises in Reckenholz (Zürich), at 47°25'37" N, 8°31'6" E. The experiment has been  
12 initiated in 1949 and comprises 12 different fertilization treatments, among which we selected  
13 three (Table 1): the control treatment (not receiving any fertilizer input), the mineral  
14 fertilization treatment (receiving yearly 139 N, 28 P, 167 K, 56 kg ha<sup>-1</sup> from 1981 and 108 N,  
15 61 P, 318 K, 12 kg ha<sup>-1</sup> in the period 1949-1980) and the farmyard manure (FYM) treatment  
16 (receiving yearly 91 N, 24 P, 65 K, 31 kg ha<sup>-1</sup> from organic fertilizer and, bi-annually, 1 t  
17 organic carbon from FYM). The site was low-intensity permanent grassland before 1949. Soil  
18 is a Luvisol (WRB, 2007), carbonate-free, with 14% clay, 27% silt and 57% sand. Organic C  
19 content was 1.3% at the beginning of the experiment, and soil pH (H<sub>2</sub>O) was 6.5. The crop  
20 rotation has a period of 8 years, and includes winter wheat/intercrop-maize-potatoes-winter  
21 wheat/intercrop-maize-summer barley-ley-ley. Main products and by-products of crops are  
22 always removed.

### 23 **2.2 Data collection and soil analyses**

24 The SOC dataset comes from Oberholzer et al. (2014). For modelling, the calibration errors  
25 for both SOC and SO<sup>14</sup>C has been expressed as coefficient of variation (CV). The CV of the  
26 SOC measurements has been measured independently in 2012 (data not published) and varied  
27 between 0.080 and 0.086 for the different treatments. The SO<sup>14</sup>C dataset comes from Leifeld  
28 and Mayer (2015). The CV in 2012 varied in this case between 0.017 and 0.029, and has been  
29 extrapolated to the whole SO<sup>14</sup>C time series. All radiocarbon concentrations utilized here are  
30 expressed in pMC as described in Stuiver and Polach (1977).



1 In the  $\text{SO}^{14}\text{C}$  time series we assumed that the pre-bomb SOC was at equilibrium with the  
2 atmospheric isotopic value. Although the  $\text{SO}^{14}\text{C}$  might slightly deviate from the  $^{14}\text{C}$  content  
3 of the atmosphere, the difference between any possible natural discrimination and the effect  
4 of the bomb peak is several orders of magnitude (Goslar *et al.*, 2004) and we regard such a  
5 difference as negligible. In order to improve the calibration of the model in respect to the  
6  $\text{SO}^{14}\text{C}$  trend, we assumed a fourth  $\text{SO}^{14}\text{C}$  point in year 1955 as corresponding to the  
7 atmospheric signature.

8 We took the atmospheric  $^{14}\text{C}$  time series from the Schauinsland station (Levin, Ingeborg and  
9 Kromer 2004; Levin *et al.*, 2013), relatively close to our site (48 km). Radiocarbon values  
10 from May to August are commonly used to represent the vegetation's signature (Levin,  
11 Ingeborg and Kromer 2004), but this implies the assumption of  $\text{CO}_2$  fixation only in late  
12 spring-summer. We calculated the difference in the time series with and without filtering out  
13 autumn-winter months, after a spline interpolation to regularize the time series, as 3.4 pMC  
14 (root mean squared error), representing a CV between 0.01 and 0.03. This we considered as  
15 negligible and used yearly averages instead.

### 16 **2.3 Calculation of C inputs**

17 The C inputs have been calculated with the C allocation coefficients proposed by Bolinder *et*  
18 *al.* (2007) and in case of potatoes by Walther *et al.* (1994). More details about the input  
19 calculations can be found in Oberholzer *et al.* (2014).

20 Carbon allocation coefficients may differ between treatments. The potential error introduced  
21 by the nonlinear nature of the root/shoot factor (Bond-Lamberty *et al.*, 2002) was considered  
22 negligible in our case due to conditions being close to optimal for plant growth at our site.  
23 The control treatment still stores as much SOC as treatments with full mineral fertilization  
24 (Oberholzer *et al.*, 2014) and it was still considered to be far from causing extreme deviations  
25 from the selected root/shoot ratio. Another source of error in our estimate is inherent to  
26 extrapolating the original root-shoot relationship (Bolinder *et al.*, 2007) to our soil. Such  
27 relationship was built on 168 samples reviewed from the literature of typical agricultural soils,  
28 not different from our alluvial soil, and this error should therefore be small. Another possible  
29 error comes from the lack of estimates for C in form of root exudates.

30 We considered the above uncertainties for the C allocation by introducing an error factor  
31 calibrated with a uniform prior distribution between 0.8 and 1.2.



1

## 2 2.4 Five possible model structures for SOC

3 The basic model (structure I) is the ICBM model developed by Andr n and K tterer (1997).  
 4 ICBM is a minimalistic model of the general SOC decomposition theory built around two  
 5 SOC pools decomposing with first order kinetics. The simplicity of the model allows for a  
 6 high degree of flexibility and makes it ideal for model structure explorations, hypotheses  
 7 testing and model development.

8 We used the model stepwise in its recursive form, as derived by K tterer *et al.* (2004), in  
 9 order to follow the highly nonlinear shape of the atmospheric <sup>14</sup>C curve of the last century  
 10 (Kurths *et al.*, 1994). The dynamic system representing SOC is described by the following  
 11 equations:

12

$$13 \quad Y_{(t)} = (Y_{(t-1)} + i_{(t-1)})e^{-k_Y r} \quad (1)$$

$$14 \quad O_{(t)} = (O_{(t-1)} + \varphi_{Y(t-1)})e^{-k_O r} + \varphi_{Y(t-1)}e^{-k_Y r} \quad (2)$$

$$15 \quad \varphi_{Y(t-1)} = h_1 \frac{k_Y (Y_{(t-1)} + i_{(t-1)})}{k_O + k_Y} \quad (3)$$

16 The SOC at time  $t$  is therefore calculated as:

$$17 \quad Tot_{(t)} = Y_{(t)} + O_{(t)} \quad (4)$$

18 This system describes the evolution of two C pools, young ( $Y$ ) and old ( $O$ ) SOC,  
 19 decomposing with rate  $k_Y$  and  $k_O$ . Their mean residence time (MRT) is defined by the  
 20 reciprocal of the decomposition constants, or  $\frac{1}{k_Y}$  and  $\frac{1}{k_O}$ . The term  $\varphi$  describes the flux

21 between the two pools, which is controlled by the humification coefficient  $h_1$  that defines the  
 22 amount of carbon that goes from  $Y$  to  $O$ . The term  $r$  aggregates climatic and edaphic  
 23 influence, and is calculated according to equations that follow in the text. The system of Eq.  
 24 (1), (2), (3) and (4) can then be modified in order to represent different hypotheses. The  
 25 model defined by the system of Eq. (1), (2), (3) and (4) is therefore calibrated for 4 unknown  
 26 parameters, namely  $k_Y$ ,  $k_O$ ,  $h_1$  and the initial distribution of C between pools  $Y$  and  $O$ .



1 A first modification (i.e. model structure II), already suggested by Juston (2012), adds a static  
 2 pool representing SOC cycling at extremely slow decomposition rates. This pool is virtually  
 3 inert and does not interact with the other pools or decomposes. Since the SOC age spectrum is  
 4 likely distributed according to a logarithmic function of age (Bosatta and Ågren, 1999), this  
 5 approximation may be reasonable for very slow SOC atoms. Eq. (4) can therefore be modified  
 6 by adding an "inert" pool  $R$  as:

$$7 \quad Tot_{(t)} = Y_{(t)} + O_{(t)} + R \quad (5)$$

8 This modification adds one parameter to the initial calibration to represent the initial value of  
 9  $R$ .

10 A second modification, i.e. model structure III, introduces instead of a static third pool a  
 11 decomposing third pool. The dynamics of the  $R$  pool in Eq. (5) now are similar to  $O$  in Eq.  
 12 (2):

$$13 \quad R_{(t)} = (R_{(t-1)} + \varphi_{O_{(t-1)}}) e^{-k_R t} + \varphi_{O_{(t-1)}} e^{-k_O t} \quad (6)$$

$$14 \quad \varphi_{O_{(t-1)}} = h_2 \frac{k_O (O_{(t-1)} + \varphi_{Y_{(t-1)}})}{k_R + k_O} \quad (7)$$

15 This modification adds two more unknown parameters to the initial model, namely  $k_R$  and  $h_2$   
 16 (table 2).

17 A third modification of structure I, i.e. model structure IV, modifies the basic set of equations  
 18 with a single, aggregated term to account for the effect of "young" substrates on microbial  
 19 dynamics and therefore on decomposition rates. We modified Eq. (1) and (2) by adding a  
 20 term  $\alpha$  in the exponent of the decomposition function according to Wutzler and Reichstein  
 21 (2013). Since the fluxes from the slower and older pool are small compared to the flux from  
 22 the younger pool we approximated the system by neglecting the former in calculating  $\alpha$  as  
 23 already suggested by Wutzler and Reichstein (2013). The resulting equation defining  $\alpha$  is:

$$24 \quad \alpha_{(t)} = \max \left( 0, 1 - \frac{\beta}{k_Y (Y_{(t)} + i_{(t)})} \right) \quad (8)$$

25 where  $\beta$  represents a lumped term aggregating microbial limitations on decomposition  
 26 (Wutzler and Reichstein 2013). The term  $\alpha$  is introduced as a modifier for both  $k_Y$  and  $k_O$ .  
 27 The denominator represents the maximum possible microbial uptake, which is the total flux





1 from  $Y$  to  $O$ . When the flux from the young pool is below the value of  $\beta$  decomposition goes  
2 to zero, but when this flux increases above this value decomposition approaches  $k_y$  and  $k_o$ .

3 This model structure adds one more unknown parameter (Table 2). Finally, model structure II  
4 was extended by a substrate control as in structure IV to give structure V. All model  
5 structures were run in annual time steps.

6 For model structures III and IV, with a substrate interaction term, an alternative MRT could  
7 be defined as  $\frac{1}{k \cdot \alpha}$ . Although, since its discussion goes beyond the scope of this manuscript,  
8 we did not consider such definition for our results, we reported it in order to better explain the  
9 numerical effect of Eq. (8) on MRT.

10

## 11 **2.5 Model structure for SO<sup>14</sup>C**

12 Each model structure was extended by running a separate system of equations for SO<sup>14</sup>C.  
13 With the introduction of SO<sup>14</sup>C, the number of parameters increases (Table 2). We calculated  
14 the ratio of <sup>12</sup>C/<sup>14</sup>C from the pMC value according to the definitions given in Stuiver and  
15 Polach (1977), and calculated from this ratio the mass of <sup>14</sup>C. We set the  $\delta^{13}\text{C}$  normalization  
16 factor at -26‰, close to that of a typical C3 soil. Most parameters were assumed to be the  
17 same as for SOC except for the initial distribution of the SO<sup>14</sup>C pools which was allowed to  
18 vary by using a normal prior distribution centered on the mean of SOC pools distribution and  
19 with a coefficient of variation of 0.1.

20 The radiocarbon decay is considered by adding the term  $\lambda$ , corresponding to  $\frac{1}{8265} \text{ yr}^{-1}$   
21 (Stuiver and Polach 1977), to all decomposition constants which then become  $k_{pool} + \lambda$ .

22 We did not consider a time lag between C assimilation and release into the SOC cycle  
23 because we are considering an agricultural system with annual plants. These plants have a  
24 physiological time lag of few hours (Kuzuyakov and Gavrichkova, 2010) and eventual storage  
25 compounds are released at the end of the cultural cycle, which is in most cases less than one  
26 year. The years during rotation where leys are present are few (Oberholzer *et al.* 2014). With  
27 the annual resolution utilized in this study the time lag could therefore considered being  
28 negligible.



1 The effect of the two data streams (SOC and  $\text{SO}^{14}\text{C}$ ) on the calibration of the model structures  
2 has been tested by introducing an arbitrary weighting term. This value, between 0 and 1, acts  
3 in the Bayesian calibration to modify the variance of the probability distributions representing  
4 the two time series. When the weighting term tends to one, the variance defining the SOC  
5 probability distribution tends to zero while for the  $\text{SO}^{14}\text{C}$  probability distribution it tends to  
6 infinite (S1). This alters the weight of that particular time series on the joint posterior  
7 distribution of the calibrated values. The precision of the  $\text{SO}^{14}\text{C}$  data stream tends to zero and  
8 so it does not influence the calibration. When the weighting tends to zero, the opposite  
9 applies.

10 In order to better capture the effect of adding the information contained in the  $\text{SO}^{14}\text{C}$  data  
11 stream in the calibration, we run all the calibrations over a gradient of such weights (with  
12 discrete values 0.05, 0.175, 0.350, 0.500, 0.650, 0.825, 0.950).

13 Since the two data streams are not homogeneous, this weighting term is considered as an  
14 empirical evaluation of the sensitivity of the model. It is an effective method for assessing the  
15 relative effect of the information from either isotope and offers more detail compared to  
16 testing only for the two options (SOC only and SOC +  $\text{SO}^{14}\text{C}$ ) separately.

17

## 18 **2.6 Considering kinetic isotope effects in soil**

19 A possible differential loss of  $\text{SO}^{14}\text{C}$  compared to SOC, caused by kinetic isotope effects  
20 (Tsai and Hu, 2013), is accounted for by the standard normalization of  $^{14}\text{C}$  values for  $\delta^{13}\text{C}$ .  
21 Since every process that possibly causes a variation of the  $^{13}\text{C}$  content from the moment that  
22 the  $\text{CO}_2$  was fixed might be assumed squared on  $^{14}\text{C}$  (Stuiver and Polach 1977), the  
23 normalization considers any process that can influence the C signature. This normalization  
24 relies on the assumption that the  $^{13}\text{C}/^{14}\text{C}$  ratio in nature is stable, since every molecule  
25 originates from atmospheric  $\text{CO}_2$  which is supposedly homogeneous in open air. The Suess  
26 effect, a change in the atmospheric isotopic composition triggered by the burning of fossil  
27 fuels (e.g. Francey *et al.*, 1999), does not represent in this sense a problem since the  $^{14}\text{C}$   
28 values are calibrated over atmospheric time series. Errors in the correction might be  
29 introduced by eventual local hot spots (e.g. industrial contaminations) for the atmospheric  
30  $^{13}\text{C}/^{14}\text{C}$  ratio. Our site, located at few kilometers from any major industry and hundreds of  
31 meters from any building, should be relatively free from local contamination sources and the  
32 closeness of the site to the measurement of atmospheric  $^{14}\text{C}$  time series should account for



1 regional variations. Nevertheless, we considered the possible error associated with these  
 2 assumptions by allowing the initial ratios of the  $^{14}\text{C}$  pools to vary slightly for  $^{14}\text{C}$  by assigning  
 3 a normal prior distribution to them, centered on the SOC ratios with deviation corresponding  
 4 to 1% of these values.

5

## 6 **2.7 Climatic and edaphic variables**

7 The parameter  $r$  in Eq. (1) and (2) in the original ICBM calibration (Andr n and K tterer,  
 8 1997) aggregates all the influences on SOC from soil type and climate. It was originally  
 9 conceived as a constant, but it has been used also as a response variable connected with  
 10 climatic and edaphic factors (Andr n *et al.*, 2012). We decided to consider  $r$  according to the  
 11 following equation:

$$12 \quad r_{(t)} = r_{Temp(t)} \cdot r_{Moist(t)} \cdot \varepsilon \quad (9)$$

13 where  $r_{Temp}$  and  $r_{Moist}$  are the decomposition rate modifiers due to temperature and soil  
 14 moisture, respectively and  $\varepsilon$  is an error term.

15 In this particular case we included proxies for soil temperature and soil moisture and we  
 16 selected the two climatic functions from the CENTURY model (Parton *et al.*, 2001; Bauer *et al.*,  
 17 2008), since they adapted well to the data available for this experiment. The temperature  
 18 function was adopted as following:

$$19 \quad r_{Temp(T)} = 0.560 + 0.465 \cdot \arctan(0.097 \cdot (T - 15 - 7)) \quad (10)$$

20 while the moisture function was adopted as following:

$$21 \quad r_{Moist(\theta)} = \left( 1 + 30e^{\left( \frac{-8.5 \cdot PPT}{PET} \right)} \right)^{-1} \quad (11)$$

22 where  $T$  is soil temperature ( $^{\circ}\text{C}$ ),  $PPT$  is the sum of stored water and precipitation, in our case  
 23 approximated to total accumulated precipitation for the reference period due to the nature of  
 24 our dataset and  $PET$  is the potential evapotranspiration (Primault, 1962). The term  $\varepsilon$  has been  
 25 described with a uniform distribution between -0.5 and +0.5.



1 Meteorological data were obtained from the Swiss Federal Research Station for Agroecology  
2 and Agriculture Zürich-Reckenholz (FAL), located at less than 100 m from the ZOFE  
3 experiment.

4 In order to maintain comparability of results with the original ICBM model,  $r$  has been  
5 normalized with its mean value as  $r_{norm(t)} = \frac{r(t)}{\bar{r}}$ , therefore making it vary around 1. The  
6 normalization, together with the introduction of the  $\varepsilon$  term in Eq. (9), reconciles the climatic  
7 functions with ICBM. The resulting variation of the  $r_{norm}$  term is pictured in S3. Since we are  
8 comparing three treatments in the same field we do not need to take into account any  
9 difference in climate between the plots, and we can use the climatic parameter only to account  
10 for variability in the data that might be due to inter-annual climatic variation.

11

## 12 **2.8 Model calibration, initialization and prior assumptions**

13 Given the close interactions between the kinetic parameters a deterministic optimization  
14 algorithm might miss possible equifinality (Beven, 2008). We therefore relied on a  
15 Metropolis-Hastings algorithm (in the implementation of JAGS, Plummer 2003), with  
16 likelihood function according to a formal Bayesian statistical framework.

17 We assumed that the parameters defining the SOC pools (namely  $k_{pool}$ ,  $h_{pool}$  and the initial  
18 pool distribution) were the same for all treatments. Every calibration has been run in 4  
19 separated Markov chains, and the convergence of the chains has been assessed visually  
20 through the use of Gelman's plots (Brooks and Gelman, 1998). Each chain was calibrated  
21 with a first adaptation period of 10.000 runs of which 5000 have been discarded as burn-in  
22 period, and then 100.000 search runs. The chains always showed reasonable convergence.

23 Priors for the rates ( $k_{pool}$ ) have been considered as normally distributed, with mean value  
24 coming from Andrén and Kätterer (1997) and deviation set to half of the mean value. The  
25 mean of the prior for  $k_o$  has been set considering it as a fixed ratio of the value of  $k_y$ . Also  
26 this ratio (0.075) has been calculated from Andrén and Kätterer (1997). The priors for  $h_y$   
27 have been considered normally distributed. Mean values to represent the different input  
28 qualities were calculated as averages of all the scenarios reported in Kätterer *et al.* (2011) as  
29 following. By assuming the composition of the young pool being similar to the inputs, we



1 chose the prior value for  $h_y$  for the control and the mineral fertilizer treatments as 0.185  
2 (which is the average for roots and shoots) while for the farmyard manure the chosen value  
3 was 0.265. We have chosen for this parameter stronger prior distributions by setting its  
4 deviation to 10% of the mean value. In the third model structure the  $h_o$  prior has been set as  
5 an uniform distribution between 0 and  $h_y$ .

6 Priors for the initial distribution of the SOC pools were considered uniformly distributed  
7 between 0 and 100% of initial SOC but constrained by the mass balance, i.e., the sum of SOC  
8 mass in all pools should add up to 100% of initial SOC. Priors for the initial distribution of  
9 the pools for  $SO^{14}C$  were generated with a uniform distribution using the portion of total SOC  
10 pools as mean and variance set to 1% of this value.

11

## 12 **2.9 Model comparison and selection**

13 Following the same principle of simplicity maximization on which we built the whole study,  
14 we selected the Akaike information criterion (AIC) to estimate the information content of the  
15 model structures. The AIC has been calculated as:

$$16 \quad AIC = 2p + n \cdot \log\left(\frac{RSS}{n}\right) \quad (12)$$

17 where  $p$  is the number of parameters,  $n$  is the number of samples and  $RSS$  is the residual sum  
18 of square of the model.

19 The use of the  $RSS$  in Eq. (12) is a simplification, since it is a metric only proportional to the  
20 likelihood. The difference lies in the lack of one integration constant. Since the AIC is used in  
21 this study only for a relative comparison between model structures, we considered this  
22 approximation justifiable. The use of the AIC rather than RMSE for measuring model  
23 performances can capture how the different model structures react to the introduction of the  
24 additional stream of information, i.e.  $SO^{14}C$ , by acting as a structure-dependent normalization,  
25 allowing for a performance comparison between different structures. Also the best weighting  
26 parameter representing the partial weight of SOC and  $SO^{14}C$  data has been selected according  
27 to the smallest AIC.

28 The choice of the AIC is motivated by its simplicity (explicit also in the intention of his  
29 author, Akaike, 1974), and by the consideration that we are comparing models over exactly



1 the same number of samples (Burnham and Anderson, 2004). But since the choice of any  
2 model performance indicator is highly subjective, we also calculated for all the models the  
3 deviance information criterion (DIC, Plummer, 2008) for comparison with the AIC.

4

### 5 **3 Results**

#### 6 **3.1 Effect of the SOC data stream on model performances**

7 In general the addition of the  $\text{SO}^{14}\text{C}$  data always improved the performance of the calibrations  
8 until a certain optimal point. This effect was similar for any of the different model structures,  
9 and an eventual relative advantage of one structure above another in considering information  
10 from  $\text{SO}^{14}\text{C}$  data was not evident. The improvement increased for every structure up to a  
11 partial weight of 0.35, and then worsened marginally when moving forward toward a higher  
12 weight of  $\text{SO}^{14}\text{C}$  data (Fig. 1). However, the decrease in performances was dramatic when  
13 moving towards a bigger relative weight of  $\text{SO}^{14}\text{C}$  data.

14 The introduction of the  $\text{SO}^{14}\text{C}$  data stream in general decreased the uncertainty of the  
15 parameters until an optimal weight for all the models without a substrate interaction  
16 (structures I, II and III), and the average coefficient of variation of the parameters followed a  
17 general pattern similar to the average AIC (S2). For the structures including substrate  
18 interaction (VI and V) the pattern was oscillating in a more complicated way, making it  
19 impossible to identify any consistent trend. The RMSE (Fig. 2) of the model structures was  
20 closely related to the AIC but with different relative values for the different structures.

21

#### 22 **3.2 Optimal model choice**

23 Overall, the "best" model structure indicated by the AIC to best describe our data was the  
24 basic ICBM, structure I (Fig. 1). This is particularly true for the FYM treatment (with highest  
25 SOC), which was the treatment best described by all our model structures.

26 The average RMSE was similar for all model structures, but there were small differences.  
27 Unexpectedly, structure III did not present the lowest average RMSE among all structures  
28 (Fig. 2), although it has the highest number of parameters. Structure II was the one which  
29 performed the best in terms of RMSE.



1 We compared these five structures also through DIC, which was 591.9 for structure I, 579.9  
2 for structure II, 593.8 for structure III, 603.1 for structure IV and 591.9 for structure V. Also  
3 the DIC indicated better performances of simpler structures and it indicated structure II as the  
4 best model. However, it did not indicate any difference between the second and third best  
5 choice (structure I and V) and differences were not as evident as when using AIC.

6

### 7 **3.3 SOC distribution and kinetics in the ZOFÉ experiment as estimated by** 8 **different model structures**

9 The MRT (Fig. 8) of the old pool, according to structures I and II, were  $94.99 \pm 0.10$  and  
10  $78.93 \pm 0.11$  years, respectively, while the ones for the young pool were  $5.91 \pm 0.09$  and  
11  $5.33 \pm 0.08$  years, respectively. Owing to the introduction of an additional term, modifying the  
12 kinetic in relation to the amount of young substrate, the results differ for structures IV and V.  
13 Here, MRT results were  $14.87 \pm 0.85$  and  $16.76 \pm 0.45$  years for the old pool and  $0.85 \pm 0.34$  and  
14  $1.01 \pm 0.30$  years for the young pool, respectively. Structure III determined pool definitions  
15 similar to structure I and II; and in this case the MRT was  $98.85 \pm 0.10$  years for the old and  
16  $4.22 \pm 0.10$  years for the young pool. The third, “recalcitrant” pool in structure III revealed a  
17 MRT of  $477.78 \pm 0.66$  years. Simulation results are shown only for structure I (Fig. 6) and II  
18 (Fig. 7), and for structure II, III and V in S5, S6 and S7.

19 The estimated size of the initial pools did not vary much among the selected model structures  
20 (Fig. 9). The amount of carbon in the young pool ranged from  $15.37 \pm 1.64$  Mg ha<sup>-1</sup> (structure  
21 I) to  $11.37 \pm 1.50$  Mg ha<sup>-1</sup> (structure III). The amount of carbon in the old pool ranged from  
22  $22.70 \pm 1.59$  Mg ha<sup>-1</sup> (structure I) to  $20.28 \pm 1.74$  Mg ha<sup>-1</sup> (structure IV) for structures  
23 considering only two pools, while it ranged from  $25.25 \pm 1.39$  Mg ha<sup>-1</sup> (structure II) to  
24  $23.00 \pm 1.70$  Mg ha<sup>-1</sup> (structure III) for structures considering three pools. As evident from  
25 Figs. 3, 4 and 5, these results are also strongly dependent on the choice of the weighting  
26 parameter between the SOC and the SO<sup>14</sup>C data streams.

27 All the tested model structures, and within all the tested values of the weighting parameter,  
28 inferred a change right after the land use change in the ZOFÉ trial. In all treatments without  
29 amendments, the young pool decreased rapidly within a few years after conversion from  
30 grassland to FYM and mineral fertilization. In structures I this decrease was more dramatic,  
31 while more complex models (II, III, IV and V) could describe the observed trends as more  
32 gradual thanks to the additional number of parameters.



1

2 **4 Discussion**3 **4.1 Effect of the C data stream on the kinetics of SOC pools**

4 During calibration all model structures seemed to react to the  $\text{SO}^{14}\text{C}$  data by reducing  
5 decomposition rates and humification coefficients, i.e., the introduction of  $\text{SO}^{14}\text{C}$  decelerated  
6 the simulated C dynamics. For structure I the effect of adding the  $\text{SO}^{14}\text{C}$  data seemed to slow  
7 down the decomposition of both pools (Fig. 3). This decrease was associated with a decrease  
8 of the humification coefficient, hence reducing also the flux of material that goes from a faster  
9 to a slower pool. In the same time the relative size of the slower pool decreased. For structure  
10 IV (Fig. 3) the addition of a substrate interaction term made the decrease in speed associated  
11 with the introduction of  $\text{SO}^{14}\text{C}$  data more dramatic and in some specific cases more difficult  
12 to interpret, but in general following a similar trend. In structures with a third inert pool, II  
13 and V (Fig. 4), trends were replicating those with only two pools. Structure V presented a  
14 pattern very similar to structure IV. The inert pool proportion increased with the increase of  
15 the weight of  $\text{SO}^{14}\text{C}$  data. Also results from structure III (S5) indicate a consistent reduction  
16 in the speed of C cycling with the introduction of the  $\text{SO}^{14}\text{C}$  data in every parameter. In  
17 general we can affirm that the inclusion of the  $\text{SO}^{14}\text{C}$  data decreased the size of the slower O  
18 pool while it increased the residence time of both Y and O pools.

19 None of our tested model structures could represent consistently both data streams at the same  
20 time. For the  $\text{SO}^{14}\text{C}$  value measured in 1973, every model structure under-predicted the  
21 isotopic value of SOC particularly for the low input treatment. Conversely, the last  $\text{SO}^{14}\text{C}$   
22 point, measured in 2012, was consistently over-predicted by every model structure. This  
23 suggests that all our model structures are still failing to represent some key process related to  
24 SOC decomposition.

25 The use of the radiocarbon bomb peak to constrain SOC turnover models, although in use  
26 since decades (Trumbore, 1989), has often raised similar controversies. The implicit inclusion  
27 of  $^{14}\text{C}$  data in C models through mass balance functions produced discrepancies between  
28 modelled and measured values in a recent study by Shirato *et al.* (2013). In another study  
29 (Rethemeyer *et al.*, 2007) this approach was judged as a viable option. The explicit  
30 consideration of  $^{14}\text{C}$  pools did not offer in this sense any advantage over implicit models.  
31 Braakhekke *et al.* (2014), using a soil profile model, found that the addition of  $\text{SO}^{14}\text{C}$  data as  
32 new constrain produced an increase in the uncertainty of the SOC stocks in the individual





1 layers, while improved just marginally the total SOC stock estimate. Ahrens *et al.* (2014)  
2 utilized  $\text{SO}^{14}\text{C}$  data to constrain an isotopically explicit single layer model in a situation  
3 where data about SOC kinetics were scarce. In that case the problem of model initialization  
4 was partially solved with additional information coming from  $^{14}\text{C}$ , but the high uncertainty of  
5 the considered system did not make it possible to determine if one site was losing or gaining  
6 carbon, and the strong interaction between MRT and deviation from the steady state made  
7 evident a trade-off between estimates with and without using  $\text{SO}^{14}\text{C}$  data.

8 One of the possible reasons for the recorded discrepancies in the estimates from models  
9 conditioned with and without  $\text{SO}^{14}\text{C}$  data might be the absence of microbial dynamics in SOC  
10 stabilization (Riley *et al.*, 2014). Ahrens *et al.* (2015), with a rather mechanistic model,  
11 recently suggested that a control on biologically mediated depolymerization can explain alone  
12 some of the observed discrepancies. But the performances of structure IV and V on our  
13 dataset, lower in terms of AIC compared to the simpler structures I and II, did not allow us to  
14 confirm such a hypothesis. Another possible explanation for the discrepancy between models  
15 and measurements is the presence of recalcitrant and old organic carbon not well captured by  
16 our model structures. Structure II was selected by the AIC, while structure III, although not  
17 performing best with AIC due to the high number of parameters, presented a good RMSE.  
18 Compared to the basic structure I both these structures introduced an additional slow SOC  
19 pool. Some form of chemical recalcitrance cannot therefore yet be ruled out.

20 In our study we focused on the optimal utilization of the information contained in  $\text{SO}^{14}\text{C}$  data  
21 together with the minimization of model complexity. We found a relevant improvement of the  
22 overall model performances when also  $\text{SO}^{14}\text{C}$  data were introduced but only until an optimal  
23 weight, while beyond that weight model performances decreased substantially. It is difficult  
24 to generalize our optimum as a general recommendation since it also depends on the density  
25 of the two data streams, but our results suggest that the relative weight of the two  
26 measurements is an additional parameter that must be considered and optimized whenever the  
27  $\text{SO}^{14}\text{C}$  data are used for model constraining.

28 A generalizable and detailed mechanistic understanding of SOC stabilization is not yet  
29 available, and SOC models are still facing a deep parametrical and structural uncertainty.  
30 According to some authors (e.g. Beven, 2002) such uncertainty is inherent to the nature of  
31 ecosystem modelling, and needs to be accepted and considered in developing new



1 methodologies. In this perspective we adopted a pragmatic approach to determine the optimal  
2 weighting factor, which turned out to be a crucial step with large impact on modelling results.

3

#### 4 **4.2 SOC dynamics in the ZOFÉ experiment as estimated by different model** 5 **structures**

6 All the model structures indicated a rapid decrease in the young pool following the conversion  
7 from grassland to cropland. This means that the annual inputs under the new management  
8 were too small to replenish the C in the former young pool while most of the material is either  
9 decomposed or humified in the old pool. This is not unlikely since also by-products, like  
10 straw, are removed, and the inputs from the cropland management are greatly reduced  
11 compared to a low-intensity grassland (Rumpel *et al.*, 2015), where a lot of the net primary  
12 productivity is either retained or returned in form of excrements. Furthermore, the disruption  
13 of the soil structure that formed under permanent grassland caused by the conversion may  
14 have released and subsequently mineralized largely undecomposed organic matter, such as  
15 particle or light fractions previously protected inside aggregates (Six and Paustian, 2014).  
16 After this re-equilibration of the young pool, the slower but constant decrease in the total SOC  
17 was explained by all the models with a slow but constant decrease in the old pool, missing the  
18 inputs previously received from a bigger young pool. All our model structures indicated that  
19 the considered treatments in the ZOFÉ experiment are all still far from a new SOC  
20 equilibrium.

21 The error in the simulated  $\text{SO}^{14}\text{C}$  might be due to an overestimation of the speed of the C  
22 cycle. Nevertheless the fact that more complex model structures (IV, V and III) did not  
23 present any advantage over simpler (I and II) structures makes it difficult to judge the weight  
24 of the two represented processes (stabilization of SOC, represented by an additional “inert”  
25 pool, or substrate feedbacks. The same discrepancy in predictions might also be caused by a  
26 systematic underestimation of the inputs. Except for the highest input treatment (FYM), the  
27 posterior probability distribution for the assumed input error term (S4) was always skewed  
28 toward the upper limit. This suggests some kind of systematic error concentrated in the lower  
29 end of the input range. Hence, the application of linear allometric functions to estimate carbon  
30 inputs from yields, as adopted here, must be treated with caution. The relatively symmetric  
31 distribution (and in general lower value) of the input error term for the FYM treatment in



1 structures I, II and III points out that model structures not considering substrate interactions  
2 might be more robust in cases of input uncertainty.

3 Another possible reason for the error in model predictions might be the nature of the error in  
4 the  $\text{SO}^{14}\text{C}$  series. This has been estimated by Leifeld and Mayer (2015) from the last time  
5 point and subsequently extrapolated to the whole time series, assuming therefore normality  
6 and homoscedasticity over time. These assumptions might not always hold in soil systems,  
7 and this would be particularly crucial in the case of the 1973 point in the control treatment.  
8 Further investigation, focused in particular to the belowground production in the ZOFÉ  
9 experiment, is needed for determining the reasons for such error.

10

#### 11 **4.3 Initial SOC distribution and MRT of SOC pools in the ZOFÉ experiment as** 12 **estimated by different model structures**

13 Our results for the kinetic parameters are in general in the same order of magnitude than what  
14 was reported in the literature (Andrén and Kätterer, 1997), although the introduction of the  
15  $\text{SO}^{14}\text{C}$  forced a deceleration of the C cycle.

16 The estimation of MRT strongly depends on all the assumptions in the model structure, and  
17 the high uncertainty around what might be the "best" structure is pointed out by the  
18 disagreement of the different criteria used for selection, which highlights the fact that there is  
19 no true model (or that "all models are wrong", Box, 1976). The combination of several  
20 structures, although difficult to perform in practice (Refsgaard *et al.*, 2006), might therefore  
21 represent a reasonable option and deserves further attention.

22 The MRT estimates (Fig. 8) depend on the introduction of a substrate control term in the  
23 model structure, but once this was accounted for it seemed quite robust. We must consider  
24 here that the introduction of a substrate control term as described by Eq. (8) modifies the  
25 definition of the decomposition constants, and therefore the MRT calculated accordingly.  
26 When introducing also the term  $\alpha$  in the calculation of MRT this ranged between 2.78 and  
27 3.13 and 46.00 and 54.47 years for young and old pool respectively, so not far from what  
28 indicated by the other structures. A detailed discussion about the MRT definition is outside  
29 the scope of this study, but here we want to make clear that a direct comparison of the MRT  
30 between these two groups of structures according to a common definition would not be  
31 meaningful and the differences in the model structure must be accounted for.



1 Model initialization seemed quite robust, with values substantially not differing between  
2 models with the same number of pools.

3

#### 4 **4.4 Balancing the bias/variance dilemma in SOC modelling**

5 As suggested by the multiple structures evaluated in this study, the conceptual nature of SOC  
6 pools makes their definition volatile. Each pool is a theoretical construction defined  
7 specifically by assumptions at the level of model structure as well as model calibration.

8 Some attempts have been made to reconcile a definition of C pools with real measurements.  
9 For example the well-established forest model Yasso (Liski *et al.*, 2005) bases its calibration  
10 on data from chemical litter fractionation, which gives the initialization values for the  
11 different C pools. But the fractionation behind Yasso might seem questionable in agricultural  
12 soils where inputs are often homogenized with the mineral fraction and less, if at all,  
13 identifiable. In more homogenized mineral topsoils the main obstacle to this approach is that  
14 available fractionation methods do not reflect precise stabilization processes (von Lützow *et*  
15 *al.*, 2007). One of the most promising recent attempts to develop a non-theoretical  
16 quantification of SOC pools in agricultural/mineral soils is the one by Zimmermann *et al.*  
17 (2007), which tried to develop a measurement standard for RothC (Coleman *et al.*, 1997)  
18 pools. All these methods share in common the risk that correlations between the  
19 measurements and the theoretical pools might be strongly localized (or difficult to reproduce,  
20 Pooplau *et al.*, 2013). This is not surprising given the complexity of SOC stabilization  
21 mechanisms (Kleber *et al.*, 2011). Indications are that stability should be considered as an  
22 intrinsic property of the soil ecosystem (Schmidt *et al.*, 2011) and thus local. It is therefore  
23 problematic to generalize a fractionation methodology that reflects in detail SOC stabilization  
24 processes, which would in turn define SOC pools.

25 Hence, we still need to aggregate the available information in a theory of SOC decomposition  
26 that is simple enough to be generalizable. This way the model structure represents the SOC  
27 decomposition processes in an aggregated (and simplified) way that is compatible with the  
28 amount of knowledge at disposal. The challenge of conciliating predictive power, and  
29 therefore practical value of our models, with accuracy is the formulation of the bias/variance  
30 trade-off as found in modern soil science.



1 As suggested from our dataset, which although not perfect is already relatively rich in  
2 information and not far from the best possible conditions available for soil carbon modelling,  
3 the information available for inverse modelling discrimination still seems insufficient to  
4 validate models that are too mechanistic.

5

## 6 **5 Conclusions**

7 The SOC in the ZOFÉ experiment underwent a profound decrease after the initial land use  
8 change from grass- to cropland. This decrease was described in the first years by all our  
9 model structures as a fast re-equilibration of the young pool, which decreased rapidly after a  
10 reduction of the inputs and/or an increased mineralization and caused in consequence a slower  
11 but constant decrease in the older pools. In the long term, treatments not receiving organic  
12 fertilization were still losing C even more than 60 years after land use change. The estimates  
13 of the MRT in the ZOFÉ experiment were robust once accounted for differences inherent to  
14 the model structures. Comparable model structures (in particular I, II and II) were relatively in  
15 agreement, and the influence of the number of pools on MRT was instead quite limited.

16 The introduction of  $SO^{14}C$  data during calibration improved performances of all model  
17 structures and reduced the uncertainty of the parametrization. It also made clear the existence  
18 of a trade-off between representing the information from  $SO^{14}C$  and SOC when utilizing a  
19 multi-pool SOC model structure. None of our five structures seemed able to reconcile  
20 consistently the two data streams. This suggests the presence of processes that were implicit  
21 in the  $SO^{14}C$  data stream but not well described in our model structures, which caused the  
22 information from the  $SO^{14}C$  to have a strong impact on the results. We therefore suggest the  
23 explicit consideration of a weight associated with each data stream as a routine procedure  
24 whenever  $SO^{14}C$  data are considered as an additional model constrain.

25 In our data set, the best model performances were achieved by the two simpler models,  
26 pointing out that the data available do not allow for a more detailed mechanistic SOC  
27 modelling. Although processes based on interactions of part of the substrate with the  
28 decomposition kinetics might explain the observations, recalcitrance inherent to the substrate  
29 (corresponding to the adoption of a slower additional decomposing C pool) remains a valid  
30 alternative in explaining the data.

31



1 **6 Data availability**

2 All the data on which this study is based are published in previous studies and the sources are  
3 cited in the text.

4

5



1 References

- 2 Ågren, G., Bosatta, E. and Balesdent, J. Isotope discrimination during decomposition of  
3 organic matter: a theoretical analysis. *Soil Science Society of America Journal*, 60, 1121–  
4 1126, 1996.
- 5 Ahrens, B., Braakhekke, M. C., Guggenberger, G., Schrumpf, M., and Reichstein, M..  
6 Contribution of sorption, DOC transport and microbial interactions to the  $^{14}\text{C}$  age of a soil  
7 organic carbon profile: Insights from a calibrated process model. *Soil Biology and*  
8 *Biochemistry*, 88, 390–402, 2015.
- 9 Ahrens, B., Reichstein, M., Borken, W., Muhr, J., Trumbore, S. E., and Wutzler, T.. Bayesian  
10 calibration of a soil organic carbon model using  $\delta^{14}\text{C}$  measurements of soil organic carbon  
11 and heterotrophic respiration as joint constraints. *Biogeosciences*, 11(8), 2147–2168, 2014.
- 12 Akaike, H. A new look at the statistical model identification. *Transactions on Automatic*  
13 *Control*, (AC-19), 716–723, 1974.
- 14 Alexander, P. Paustian, K., Smith, P., Moran, D.. The economics of soil C sequestration and  
15 agricultural emissions abatement. *Soil*, 1(1), 331–339, 2015.
- 16 Andrén, O., Kätterer, T., Juston, J., Waswa, B., and De Nowina, K. R.. Soil carbon dynamics ,  
17 climate , crops and soil type – calculations using introductory carbon balance model ( ICBM )  
18 and agricultural field trial data from sub-Saharan Africa. *African Journal of Agricultural*  
19 *Research*, 7(43), 5800–5809, 2012.
- 20 Andrén, O. and Kätterer, T.. ICBM : The Introductory Carbon Balance Model for Exploration  
21 of Soil Carbon Balances. *Ecological Applications*, 7(4), 1226–1236, 1997.
- 22 Bauer, J., Herbst, M., Huisman, J., Weihermüller, L., Vereecken, H.. Sensitivity of simulated  
23 soil heterotrophic respiration to temperature and moisture reduction functions. *Geoderma*,  
24 145(1-2), 17–27, 2008.
- 25 Beven, K. A manifesto for the equifinality thesis. *Journal of Hydrology*, 320(1-2), 18–36,  
26 2006.
- 27 Beven, K.. Towards a coherent philosophy for modelling the environment. *Proceedings of the*  
28 *Royal Society A: Mathematical, Physical and Engineering Sciences*, 458(2026), 2465–2484,  
29 2002.



- 1 Beven, K.J.. Environmental Modelling: An Uncertain Future?, London: Routledge, 2008.
- 2 Bolinder, M. a. et al.. An approach for estimating net primary productivity and annual carbon  
3 inputs to soil for common agricultural crops in Canada. Agriculture, Ecosystems and  
4 Environment, 118(1-4), 29–42, 2007.
- 5 Bond-Lamberty, B., Wang, C. and Gower, S.T.. Aboveground and belowground biomass and  
6 sapwood area allometric equations for six boreal tree species of northern Manitoba. Canadian  
7 Journal of Forest Research, 32, 1441–1450, 2002.
- 8 Bosatta, E. and Ågren, G.. Soil organic matter quality interpreted thermodynamically. Soil  
9 Biology and Biochemistry, 31, 1889–1891, 1999.
- 10 Box, G.E.P.. Science and Statistics. Journal of the American Statistical Association, 71(356),  
11 791–799, 1976.
- 12 Braakhekke, M. C., Beer, C., Schrumppf, M., Ekici, A., Ahrens, B., Hoosbeek, M. R., Kruijt,  
13 B., Kabat, P., Reichstein, M.. The use of radiocarbon to constrain current and future soil  
14 organic matter turnover and transport in a temperate forest. Journal of Geophysical Research:  
15 Biogeosciences, 119(3), 372–391, 2014.
- 16 Briscoe, E. and Feldman, J. Conceptual complexity and the bias/variance tradeoff. Cognition,  
17 118(1), 2–16, 2011.
- 18 Brooks, S. P. B., and Gelman, A. G.. General methods for monitoring convergence of  
19 iterative simulations. Journal of Computational and Graphical Statistics, 7(4), 434–455, 1998.
- 20 Burnham, K.P. and Anderson, D.R.. Multimodel Inference: Understanding AIC and BIC in  
21 Model Selection. Sociological Methods and Research, 33(2), 261–304, 2004.
- 22 Coleman, K., Jenkinson, D. and Crocker, G.. Simulating trends in soil organic carbon in long-  
23 term experiments using RothC-26.3. Geoderma, 81, 29–44, 1997.
- 24 Francey, R., Allison, C., Etheridge, D., Trudinger, C., Enting, I., Leuenberg, M., Lagenfelds,  
25 R., Michel, E., Steele, L.. A 1000-year high precision record of  $\delta^{13}\text{C}$  in atmospheric  $\text{CO}_2$ .  
26 Tellus, 51b, 170–193, 1999.
- 27 Goslar, T., Van Der Knaap, W., Hicks, S., Andric, M., Czernik, J., Goslar, E., Räsänen, S.,  
28 Hyötylä, H.. Radiocarbon dating of modern peat profiles: pre- and post-bomb C variations in  
29 the construction of age–depth models. Radiocarbon, 46(1), 1111–1150, 2004.





- 1 IPCC. Climate Change 2014: Impacts, Adaptation, and Vulnerability. Part A: Global and  
2 Sectoral Aspects. . Contribution of Working Group II to the Fifth Assessment Report of the  
3 Intergovernmental Panel on Climate Change C. B. Field et al., eds., Cambridge, United  
4 Kingdom and New York, NY, USA: Cambridge University Press, 2014.
- 5 Juston, J.. Environmental Modelling: Learning from Uncertainty, TRITA LWR PHD 1068,  
6 2012
- 7 Kätterer, T., Bolinder, M., Andrén, O., Kirchmann, H., and Menichetti, L.. Roots contribute  
8 more to refractory soil organic matter than aboveground crop residues, as revealed by a long-  
9 term field experiment. *Agriculture Ecosystems and Environment*, 141, 184–192, 2011.
- 10 Kätterer, T. and Andrén, O.. The ICBM family of analytically solved models of soil carbon,  
11 nitrogen and microbial biomass dynamics – descriptions and application examples. *Ecological*  
12 *Modelling*, 136, 191–207, 2001.
- 13 Kätterer, T., Andrén, O. and Persson, J.. The impact of altered management on long-term  
14 agricultural soil carbon stocks – a Swedish case study. *Nutrient Cycling in Agroecosystems*,  
15 70, 179–188, 2004.
- 16 Kleber, M., Nico, P. S., Plante, A., Filley, T., Kramer, M., Swanston, C., and Sollins, P.. Old  
17 and stable soil organic matter is not necessarily chemically recalcitrant: implications for  
18 modelling concepts and temperature sensitivity. *Global Change Biology*, 17(2), 1097–1107,  
19 2011.
- 20 Kurths, J., Schwarz, U., Sonett, C. P., and Parlitz, U.. Testing for nonlinearity in radiocarbon  
21 data. *Nonlinear Processes in Geophysics*, 1(1), 72–76, 1994.
- 22 Kuzyakov, Y., and Gavrichkova, O.. Time lag between photosynthesis and carbon dioxide  
23 efflux from soil: A review of mechanisms and controls. *Global Change Biology*, 16(12),  
24 3386–3406, 2010.
- 25 Lal, R.. Soil carbon sequestration to mitigate climate change. *Geoderma*, 123(1-2), pp.1–22,  
26 2004
- 27 Leifeld, J.. Biased <sup>14</sup>C-derived organic carbon turnover estimates following black carbon  
28 input to soil: an exploration with RothC. *Biogeochemistry*, 88(3), pp.205–211, 2008.



- 1 Leifeld, J. and Mayer, J..  $^{14}\text{C}$  in cropland soil of a long-term field trial – in-field variability  
2 and implications for estimating carbon turnover. *SOIL Discussions*, 2(1),217–231, 2015.  
3 Available at: <http://www.soil-discuss.net/2/217/2015/>.
- 4 Levin, I., Kromer, B. and Hammer, S.. Atmospheric  $\Delta^{14}\text{CO}_2$  trend in Western European  
5 background air from 2000 to 2012. *Tellus B*, 1, 1–7, 2013.
- 6 Levin, Ingeborg and Kromer, B.. The tropospheric  $^{14}\text{CO}_2$  level in mid-latitudes of the  
7 Northern Hemisphere (1959–2003). *Radiocarbon*, 46(3), pp.1261–1272, 2004.
- 8 Liski, J., Palosuo, T., Peltoniemi, M., and Sievänen, R.. Carbon and decomposition model  
9 Yasso for forest soils. *Ecological Modelling*, 189(1-2), 168–182, 2005.
- 10 von Lützw, M., Kögel-Knabner, I., Ekschmitt, K., Flessa, H., Guggenberger, G., Matzner,  
11 E., and Marschner, B.. SOM fractionation methods: Relevance to functional pools and to  
12 stabilization mechanisms. *Soil Biology and Biochemistry*, 39(9), 2183–2207, 2007.
- 13 Oberholzer, H.R., Leifeld, J. and Mayer, J.. Changes in soil carbon and crop yield over 60  
14 years in the Zürich Organic Fertilization Experiment , following land-use change from  
15 grassland to cropland. *Journal of Plant Nutrition and Soil Science*, 493, 696–704, 2014.
- 16 Parton, B., Ojima, D., Del Grosso, S., and Keough, C.. CENTURY Tutorial. Supplement to  
17 CENTURY User’s Manual, 2001.
- 18 Parton, W. J., Scurlock, J. M. O., Ojima, D. S., Gilmanov, T. G., Scholes, R. J., Schimel, D.  
19 S., Kirchner, T., Menaut, J-C., Seastedt, T., Garcia Moya, E. G., Kamnalrut, A., Kinyamario,  
20 J. I. Observations and modeling of biomass and soil organic matter dynamics for the  
21 grassland biome worldwide. *Global Biogeochemical Cycles*, 7(4), 785–809, 1993.
- 22 Plummer, M.. JAGS : A Program for Analysis of Bayesian Graphical Models Using Gibbs  
23 Sampling JAGS : Just Another Gibbs Sampler. In K. Hornik, F. Leisch, and A. Zeileis, eds.  
24 Proceedings of the 3rd International Workshop on Distributed Statistical Computing. Vienna,  
25 2003.
- 26 Plummer, M.. Penalized loss functions for Bayesian model comparison. *Biostatistics*, 9(3),  
27 523–539, 2008.
- 28 Poeplau, C., Don, a., Dondini, M., Leifeld, J., Nemo, R., Schumacher, J., Senapati, N.,  
29 Wiesmeier, M.. Reproducibility of a soil organic carbon fractionation method to derive RothC  
30 carbon pools. *European Journal of Soil Science*, 64(6), 735–746, 2013.



- 1 Primault, B.. Du calcul de l'évapotranspiration. Arch. Met. Geoph. Biocl. Series B, 12, 124–  
2 150, 1962.
- 3 Refsgaard, J. C., van der Sluijs, J. P., Brown, J., and van der Keur, P.. A framework for  
4 dealing with uncertainty due to model structure error. Advances in Water Resources, 29(11),  
5 1586–1597, 2006.
- 6 Rethemeyer, J., Grootes, P. M., Brodowski, S., and Ludwig, B.. Evaluation of soil <sup>14</sup>C data for  
7 estimating inert organic matter in the RothC model. Radiocarbon, 49(2), 1079–1091, 2007.
- 8 Riley, W. J., Maggi, F. M., Kleber, M., Torn, M. S., Tang, J. Y., Dwivedi, D., & Guerry, N..  
9 Long residence times of rapidly decomposable soil organic matter: application of a multi-  
10 phase, multi-component, and vertically-resolved model (BAMS1) to soil carbon dynamics.  
11 Geoscientific Model Development, 7(1), 1335–1355, 2014.
- 12 Rumpel, C., Crème, A., Ngo, P. T., Velásquez, G., Mora, M. L., and Chabbi, A.. The impact  
13 of grassland management on biogeochemical cycles involving carbon, nitrogen and  
14 phosphorus. Journal of Soil Science and Plant Nutrition, 15(2), 353-371, 2015.
- 15 Schimel, J. and Weintraub, M.. The implications of exoenzyme activity on microbial carbon  
16 and nitrogen limitation in soil: a theoretical model. Soil Biology and Biochemistry, 35, 549–  
17 563, 2003.
- 18 Schmidt, M., Torn, M., Abiven, S., Dittmar, T., Guggenberger, G., Janssens, I., Kleber, M.,  
19 Kögel-Knabner, I., Lehmann, J., Manning, D., Nannipieri, P., Rasse, D., Weiner, S.,  
20 Trumbore, S.. Persistence of soil organic matter as an ecosystem property. Nature, 478, 49–  
21 56, 2011.
- 22 Shirato, Y., Jomura, M., Wagai, R., Kondo, M., Tanabe, K., and Uchida, M.. Deviations  
23 between observed and RothC-simulated  $\Delta^{14}\text{C}$  values despite improved IOM initialization.  
24 European Journal of Soil Science, 64(5), 576–585, 2013.
- 25 Six, J. and Paustian, K.. Aggregate-associated soil organic matter as an ecosystem property  
26 and a measurement tool. Soil Biology and Biochemistry, 68, A4–A9, 2014.
- 27 Stuiver, M. and Polach, H.. Reporting of <sup>14</sup>C Data. Radiocarbon, 19(3), 355–363, 1977.
- 28 Trumbore, S.. AMS <sup>14</sup>C measurements of fractionated soil organic-matter-an approach to  
29 deciphering the soil carbon-cycle. Radiocarbon, 31, 644–654, 1989.



- 1 Trumbore, S.E. and Czimczik, C.I. An uncertain future for soil carbon. *Science*,  
2 321(September), 1455–1456, 2008.
- 3 Tsai, W-C., and Hu, W-P.. Theoretical analysis on the kinetic isotope effects of bimolecular  
4 nucleophilic substitution  $S_N2$  reactions and their temperature dependence. *Molecules*, 18(4),  
5 4816–43, 2013.
- 6 Walther, U., Menzi, H., Ryser, J.-P., Flisch, R., Jeangros, B., Kessler, W., Maillard, A.,  
7 Siegenthaler, A. F., Vuilloud, P. A.. Grund-lagen für die Düngung im Acker- und Futterbau.  
8 *Agrarforschung*, 1, 1–40, 1994.
- 9 WRB, I.W.G.. World Reference Base for Soil Resources 2006, first update 2007. *World Soil*  
10 *Resources Reports No. 103*. FAO, Rome, 2007.
- 11 Wutzler, T. and Reichstein, M.. Priming and substrate quality interactions in soil organic  
12 matter models. *Biogeosciences*, 10(3), 2089–2103, 2013.
- 13 Zimmermann, M., Leifeld, J., Schmidt, M. W. I., Smith, P., and Fuhrer, J.. Measured soil  
14 organic matter fractions can be related to pools in the RothC model. *European Journal of Soil*  
15 *Science*, 58(3), 658–667, 2007.
- 16
- 17



- 1 Table 1: The treatments considered in this study. † = kg ha<sup>-1</sup> y<sup>-1</sup>, †† = Mg ha<sup>-1</sup> y<sup>-1</sup>, \* = from  
 2 organic amendment. <sup>a</sup>=1949-1980, <sup>b</sup>=since 1981, <sup>c</sup>=1949-1990, <sup>d</sup>=since 1991 \* = average.

Treatment	Annual input					Fertilizer C <sup>†</sup>	Estimated total C <sup>†</sup>	Initial SOC <sup>††</sup>	Final SOC <sup>††</sup>
	N <sup>†</sup>	P <sup>†</sup>	K <sup>†</sup>	Mg <sup>†</sup>					
Control		0	0	0	0	0	580	38.75	24.28
N2P2K2Mg	108 <sup>a</sup> /139 <sup>b</sup>	61 <sup>c</sup> /38 <sup>d</sup>	318 <sup>c</sup> /167 <sup>d</sup>	12 <sup>a</sup> /56 <sup>b</sup>		0	1350	38.75	27.05
Farmyard Manure	91*	24*	65*	31	2500		3621	38.75	31.70

3

- 4 Table 2: Summary of the model structures tested in this study (considered here in their basic  
 5 forms for total C only and for the two isotopes together.

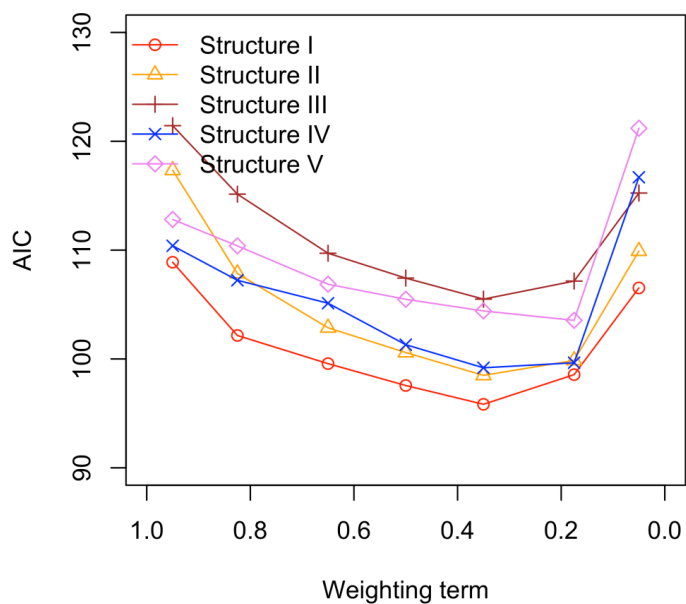
	Struct. I	Struct. II	Struct. III	Struct. IV	Struct. V
Description	Two pools	Two pools + Inert	Three pools	Two pools + substrate control	Two pools + substrate control + Inert
Parameters (SOC)	4	5	7	5	6
Parameters (SOC+SO <sup>14</sup> C)	4+1	5+2	7+3	5+1	6+2

6

7



1  
2

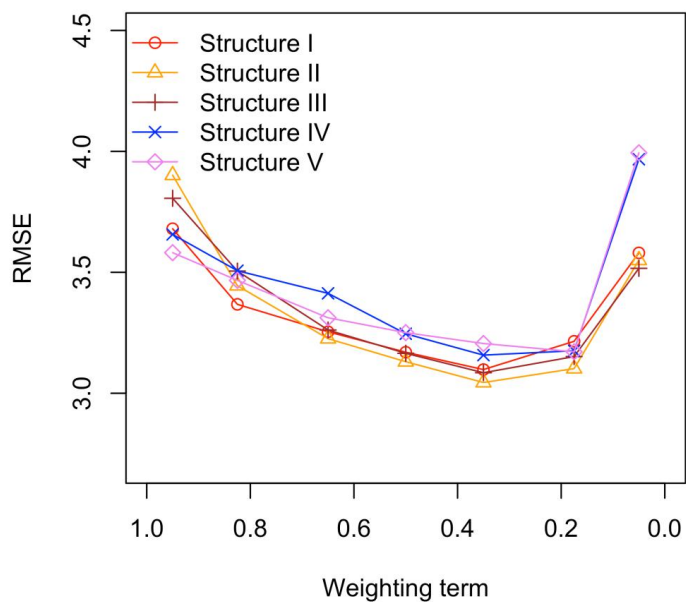


3  
4  
5  
6

Figure 1: Average of the AIC among all the three treatments for the five model structures with the variation of the relative weight of  $\text{SO}^{14}\text{C}$  over total C. In this scale 1 means only total C, 0 means only  $\text{SO}^{14}\text{C}$ .

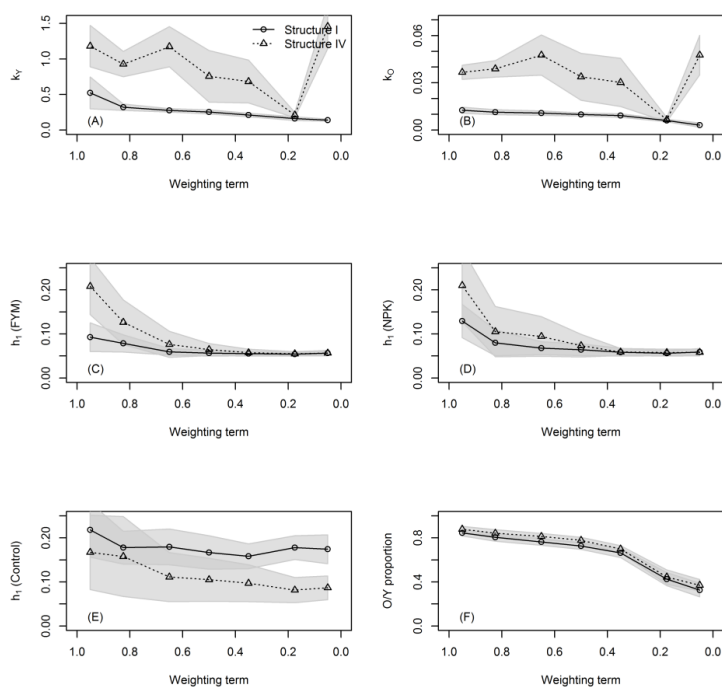


1  
2



3  
4  
5  
6

Figure 2: Average of the RMSE among all the three treatments for the five model structures with the variation of the relative weight of  $\text{SO}^{14}\text{C}$  over total C. In this scale 1 means only total C, 0 means only  $\text{SO}^{14}\text{C}$ .

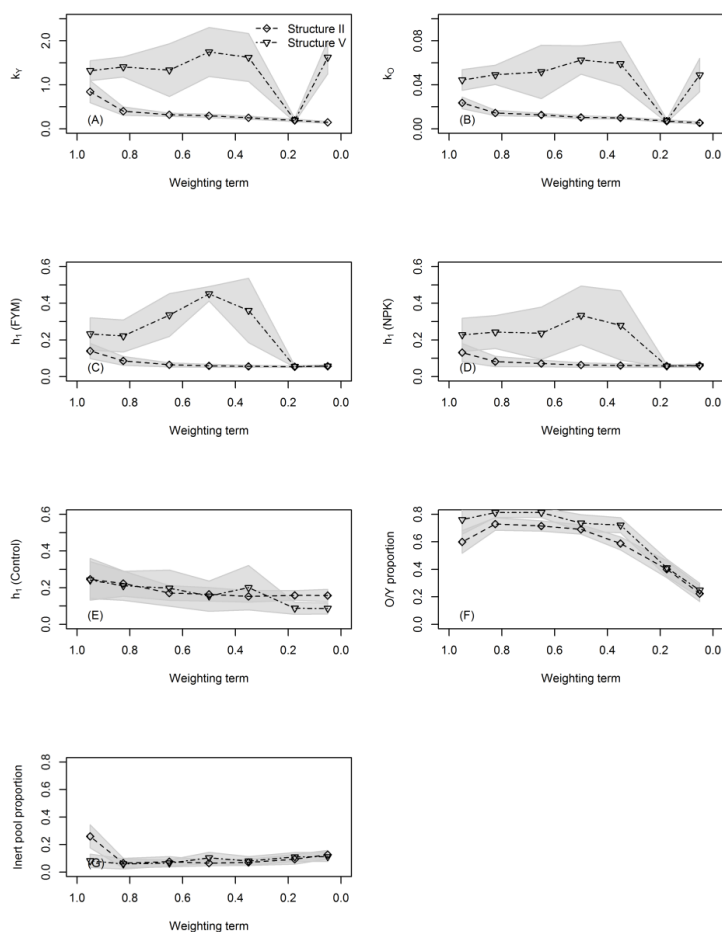


1  
 2 Figure 3: Effect of the  $SO^{14}C$  stream over the main SOC parameters in structures I and IV. In this scale 1 means  
 3 only total C, 0 means only  $SO^{14}C$ . The shaded areas represent the error of the calibrated parameter (calculated as  
 4 standard deviation of the whole Markov chain).  
 5





1



2

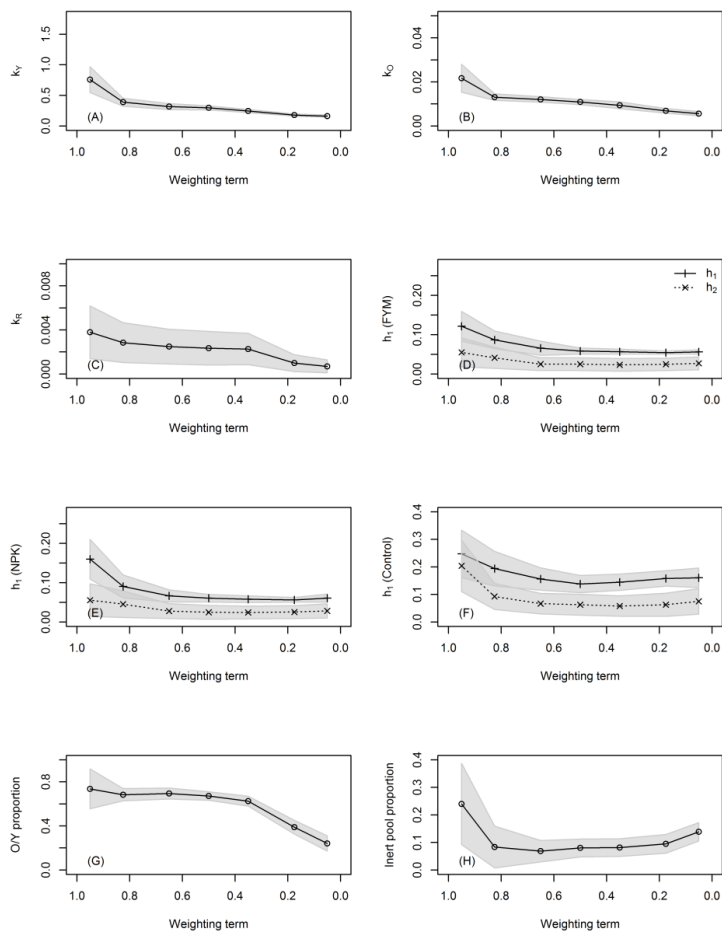
3

4

5

6

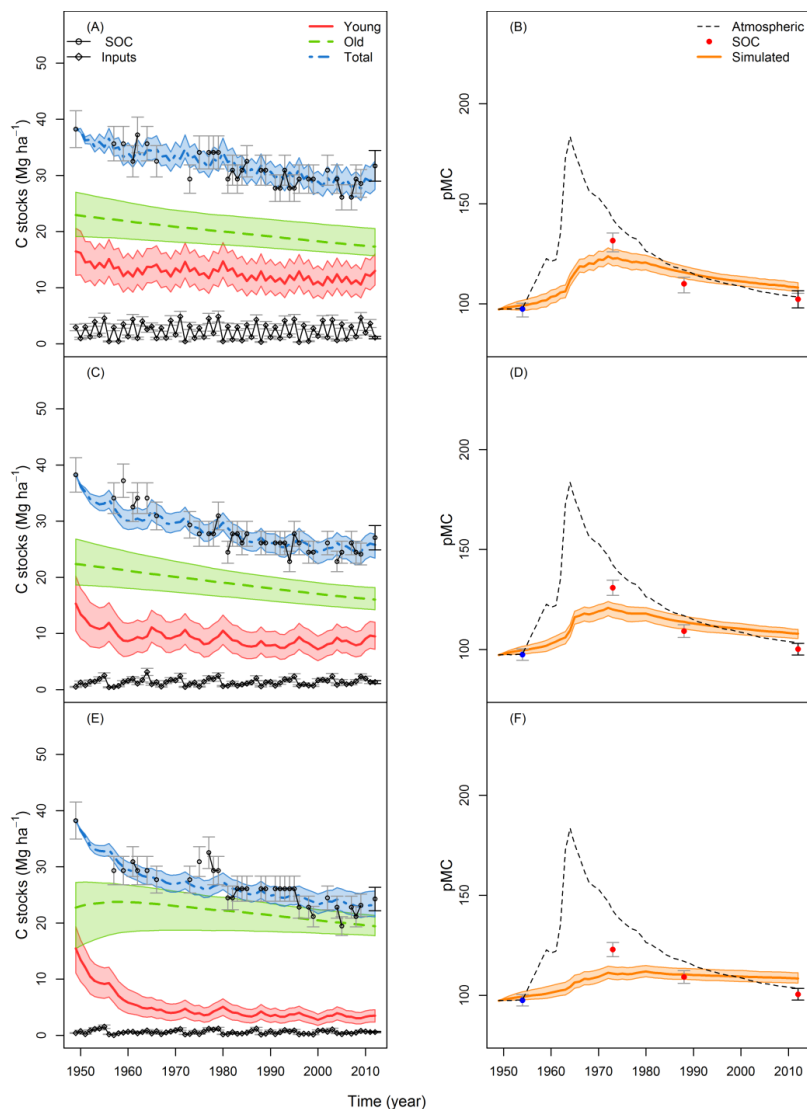
Figure 4: Effect of the  $SO^{14}C$  data over the main SOC parameters in structure II and V. In this scale 1 means only total C, 0 means only  $SO^{14}C$ . The shaded areas represent the error of the calibrated parameter (calculated as standard deviation of the whole Markov chain).



1

2 Figure 5: Effect of the  $SO^{14}C$  data over the main SOC parameters in structure III. In this scale 1 means only total  
 3 C, 0 means only  $SO^{14}C$ . The shaded areas represent the error of the calibrated parameter (calculated as standard  
 4 deviation of the whole Markov chain).

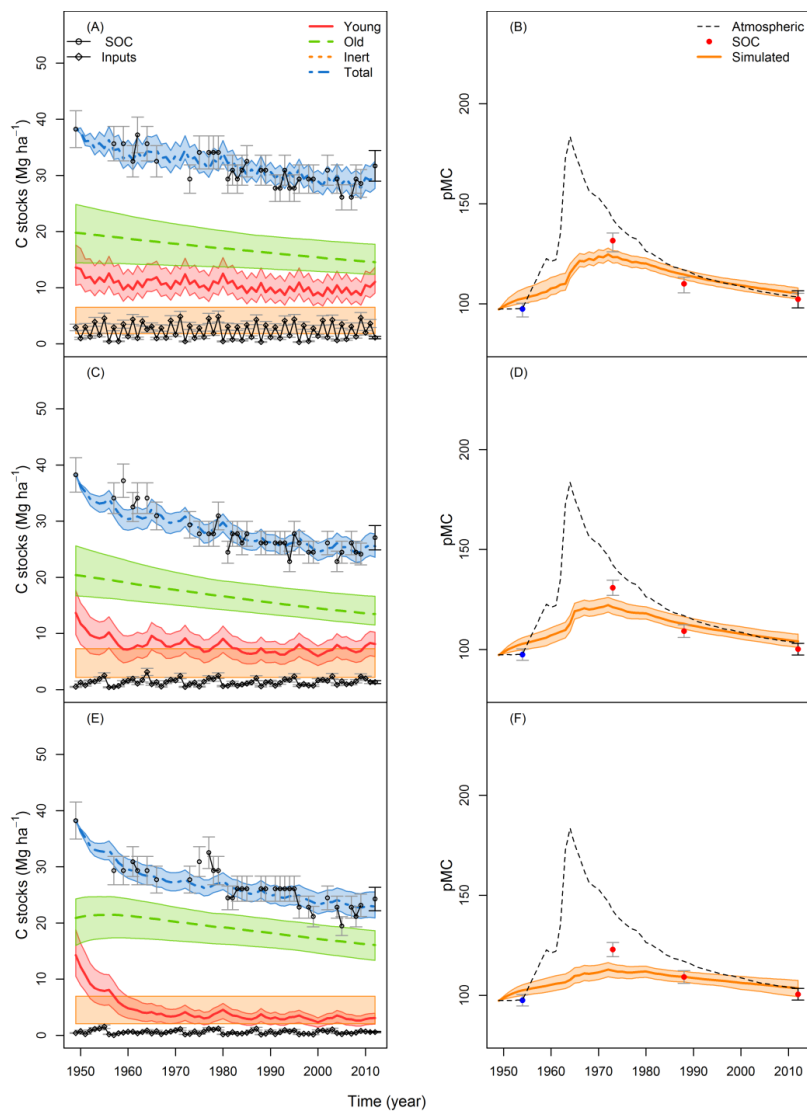
5



1

2 Figure 6: Simulation of SOC pools in the ZOFÉ trial as described by model structure I, with weighting factor =  
 3 0.35. Error bars represent the measured (black) and estimated (dark grey) standard error of the measurements.  
 4 SOC (A,C,E) is in Mg ha<sup>-1</sup>, while SO<sup>14</sup>C (B, D, F) is in pMC.

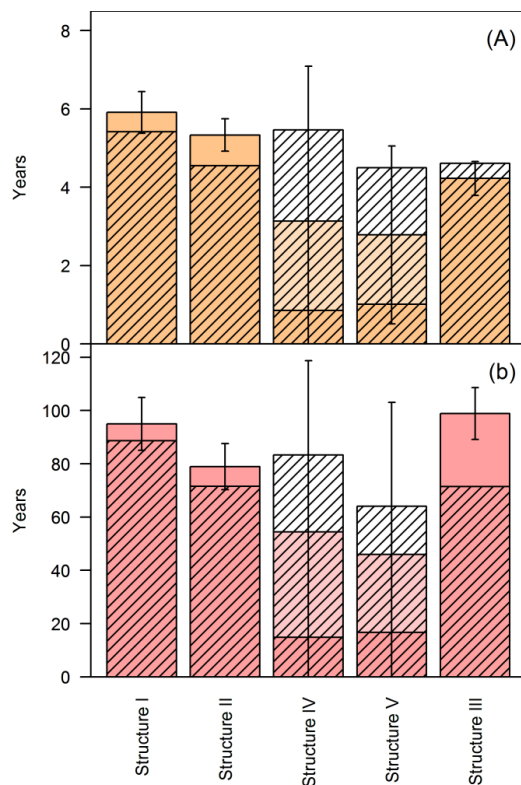
5



1

2 Figure 7: Simulation of SOC pools in the ZOFÉ trial as described by model structure II, with weighting factor =  
 3 0.35. Error bars represent the measured (black) and estimated (dark grey) standard error of the measurements.  
 4 SOC (A,C,E) is in Mg ha<sup>-1</sup>, while SO<sup>14</sup>C (B, D, F) is in pMC.

5



1

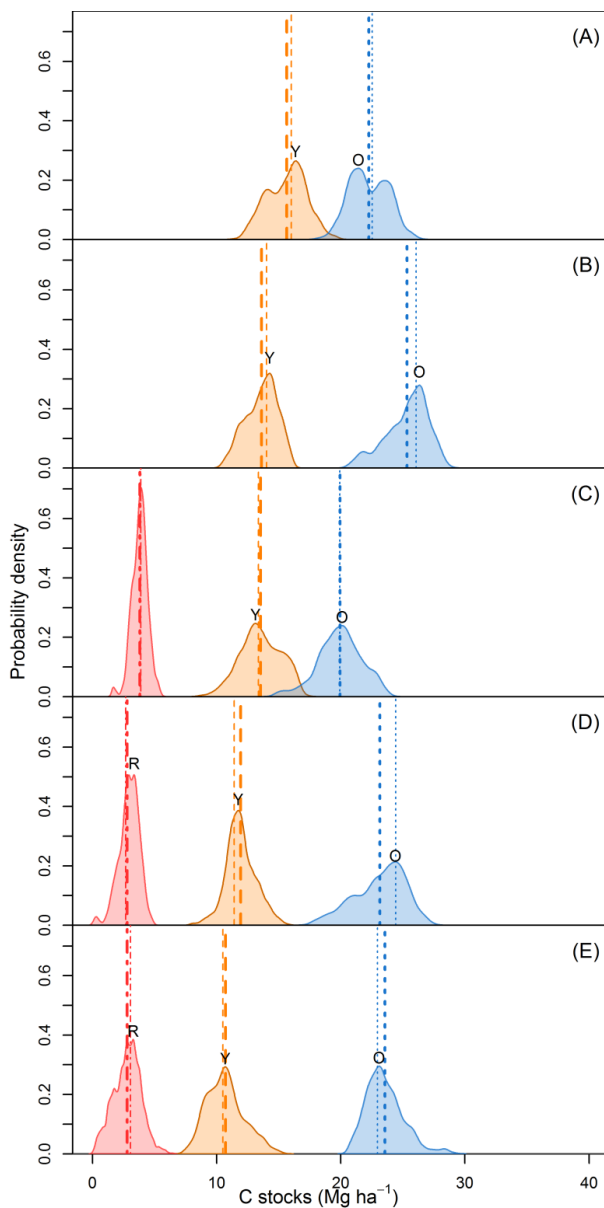
2 Figure 8: MRT of the young pool (A) and old pool (B) of SOC in the ZOFÉ trial as indicated by the model  
 3 structures examined, with weighting factor = 0.35 (solid colored area) and weighting factor = 0.65 (shaded area).

4 The solid lighter colored area denotes the MRT calculated (for structures IV and V) according to  $\frac{1}{k \cdot \alpha}$ , while

5 the darker colored area according to  $\frac{1}{k}$ , Error bars, reported only for weighting factor = 0.35 for readability

6 reasons, denote the error of the estimate calculated as standard deviation of the whole Markov chain and depends  
 7 on the model structure, model assumptions and priors.

8



1  
 2 Figure 9: Probability distribution of the initial size of the C pools (Y=Young, O=Old, R=Recalcitrant) in  
 3 structure I (A), IV (B), II (C) and V (D), with weighting factor = 0.35. On the vertical axis is depicted the  
 4 probability density of the parameter (dimensionless) and on the horizontal axis the value of the parameter (in Mg  
 5 ha<sup>-1</sup>). Vertical lines are representing the mean value (thick lines) and the Venter estimated mode (thin lines) of  
 6 the Markov chains.

7  
 8